Sensing and regulation of long-chain polyunsaturated fatty acids pool in marine mollusks : Characterization of UBXD8 from the razor clam Sinonovacula constricta

Biochimica et Biophysica Acta - Molecular and Cell Biology of Lipids
Ran, Zhaoshou; Xie, Haixuan; Tian, Xuxu; Kong, Fei; Liao, Kai et al
https://doi.org/10.1016/j.bbalip.2023.159448

BBA - Molecular and Cell Biology of Lipids 1869 (2024) 159448

Contents lists available at ScienceDirect

BBA - Molecular and Cell Biology of Lipids

journal homepage: www.elsevier.com/locate/bbalip

Sensing and regulation of long-chain polyunsaturated fatty acids pool in marine mollusks: Characterization of UBXD8 from the razor clam *Sinonovacula constricta*

Zhaoshou Ran [a,b,d,*], Haixuan Xie [a], Xuxu Tian [a], Fei Kong [a], Kai Liao [a], Xiaojun Yan [b], Jilin Xu [a,b,c,*]

[a] Key Laboratory of Aquacultural Biotechnology Ministry of Education, Ningbo University, Ningbo, Zhejiang 315211, China
[b] Key Laboratory of Marine Biotechnology of Zhejiang Province, Ningbo, Zhejiang 315211, China
[c] Fujian Dalai Seedling Technology Co., Ltd., Luoyuan, Fujian 350600, China
[d] Nutrition, Metabolism and Genomics Group, Division of Human Nutrition and Health, Wageningen University, the Netherlands

ARTICLE INFO

Keywords:
Long-chain polyunsaturated fatty acids
Biosynthesis
Regulation
Homeostasis
Marine mollusks

ABSTRACT

The razor clam *Sinonovacula constricta* is known for its richness in long-chain polyunsaturated fatty acids (LC-PUFA, C ≥ 20). Previously, we demonstrated that it possesses a complete LC-PUFA biosynthetic pathway. However, the mechanisms by which it senses the LC-PUFA pool to regulate their biosynthesis remain unclear. Here, we presented the LC-PUFA sensor UBXD8 as a critical molecule in this intriguing process. The *S. constricta* UBXD8 (*Sc*UBXD8) shared all characteristic features of its mammalian counterpart and exhibited high mRNA levels in digestive tissues, suggesting its functional role in this bivalve species. By purification of *Sc*UBXD8 protein *in vitro*, we discovered its ability to sense unsaturated fatty acids (UFA, C ≥ 14) but not saturated ones, as evidenced by polymerization detection. Furthermore, the intensity of *Sc*UBXD8 polymerization increased progressively with longer acyl chain lengths, greater unsaturation degrees, and higher UFA concentrations. Exceptionally, for those located at the same node in LC-PUFA biosynthetic pathway, *Sc*UBXD8 displayed a stronger sensitivity to n-6 UFA compared to n-3 UFA. These results suggested a critical role for *Sc*UBXD8 in balancing fatty acids composition and ratio of n-6/n-3 UFA in *S. constricta*. Moreover, the UAS domain was confirmed essential for *Sc*UBXD8 polymerization. Through knockdown of *Sc*Ubxd8 gene *in vivo*, there were significant shifts in expression patterns of genes related to LC-PUFA biosynthesis, concurrently influencing fatty acids compositions. These results suggested that *Sc*UBXD8 likely plays a regulatory role in LC-PUFA biosynthesis, possibly through the INSIG-SREBP pathway. Collectively, this study proposed that *S. constricta* might maintain LC-PUFA homeostasis through UBXD8 to regulate their biosynthesis.

1. Introduction

Marine mollusks are excellent resources of long-chain polyunsaturated fatty acids (LC-PUFA, C ≥ 20, carbon bonds≥2), such as arachidonic acid (20:4n-6, ARA), eicosapentaenoic acid (20:5n-3, EPA), and docosahexaenoic acid (22:6n-3, DHA) [1]. These fatty acids (FA) are significant for human health in various physiological processes, including cell membrane structure and function, inflammation regulation, and brain development [2]. Consequently, in the past decade, there has been extensive research into the molecular mechanisms of LC-PUFA biosynthesis in marine mollusks [3]. Specifically, the critical enzymes associated with LC-PUFA biosynthesis, including fatty acyl desaturases (Fads) and elongases of very long chain fatty acids (Elovls), have been identified and functionally characterized in many economically significant species [3]. These species include the cephalopods such as *Octopus vulgaris* [4–7] and *Sepia officinalis* [8], the gastropods like *Haliotis discus hannai* [9], and the bivalves including *Chlamys nobilis* [10–12], *Crassostrea angulate* [13], and *Ruditapes philippinarum* [14]. In contrast, progress in understanding the regulatory mechanisms of LC-PUFA biosynthesis has been slow [15,16]. Particularly, the mechanisms by which marine mollusks sense LC-PUFA pool to keep homeostasis, thereby regulating LC-PUFA biosynthesis are poorly understood.

* Corresponding authors at: Ningbo University, Ningbo, Zhejiang 315211, China.
E-mail addresses: ranzhaoshou@nbu.edu.cn (Z. Ran), xujilin@nbu.edu.cn (J. Xu).

https://doi.org/10.1016/j.bbalip.2023.159448
Received 25 August 2023; Received in revised form 17 December 2023; Accepted 26 December 2023
Available online 4 January 2024

In mammals, the ubiquitin regulatory X domain containing protein 8 (UBXD8) has been identified as a sensor for unsaturated fatty acids (UFA) that plays a critical role in LC-PUFA homeostasis by regulating the maturation of sterol-regulatory element binding protein (SREBP)-1 [17–19], which is a pivotal transcriptional factor in regulating LC-PUFA biosynthesis [20]. Specifically, UBXD8 is a multi-domain protein containing a UBX domain that interacts with p97 [21], a UBA domain that binds polyubiquitin chains [21], and a UAS domain that interacts with UFA [19]. When cells lack UFA, the low level of UFA is sensed by the UAS domain of UBXD8, leading to the degradation of insulin induced gene (INSIG)-1 through the cooperation of the UBX and UBA domains. This, in turn, results in the maturation of SREBP-1 by the enzymes S1P and S2P [17,18]. Conversely, when cells are rich in UFA, the high level of UFA is sensed by the UAS domain of UBXD8. This leads to the polymerization and inactivation of UBXD8, which subsequently blocks SREBP maturation [17,18]. Importantly, although UBXD8 has long been known as a sensor for UFA and a regulator in LC-PUFA biosynthesis in mammal cells [17–19], the complete repertoire of its sensitivities towards different FA is not well understood, and its role in living mammals/animals remains to be determined. Furthermore, its corresponding roles in aquatic animals, including marine mollusks, remain a mystery.

The razor clam *Sinonovacula constricta* (Lamarck 1818) is a well-known bivalve species that is widely cultured in China, Korea, and Japan, possessing significant economic and nutritional value [22]. Notably, *S. constricta* is not only rich in LC-PUFA such as EPA and DHA (each accounting for approximately 10 % of total FA, approximately 3.5 $\mu g \cdot mg^{-1}$ dry weight) [23], but it has also been demonstrated to be the first marine mollusk to possess the complete LC-PUFA biosynthetic pathway [24,25]. This pathway includes two Δ5 Fads (a and b), one Δ6 Fad [24], one Elovl2/5, two Elovl4 (a and b), and one novel Elovl with Elovl4 activity (Elovlc) [25]. Specifically, *S. constricta*'s Δ5 Fad catalyzes the conversion of 20:3n-6 and 20:4n-3 into ARA and EPA, respectively [24]. *S. constricta*'s Δ6 Fad is not only responsible for the desaturation of 18:2n-6 (LA) and 18:3n-3 (ALA) to yield 18:3n-6 and 18:4n-3 [24] but also exhibits the capacity to desaturate 24:5n-3, generating 24:6n-3 [25]. This 24:6n-3 is then partially subjected to β-oxidation, leading to the production of DHA. *S. constricta*'s Elovl2/5 demonstrates high elongation activity towards C18–20 FA, while Elovl4 transcripts exhibit a strong preference for elongating C $\geq$ 22 FA [25]. Furthermore, *S. constricta* has been a focus of research as the regulation of LC-PUFA biosynthesis in marine mollusks [15]. Specifically, the transcription of the *S. constricta* Δ6 Fad is controlled by SREBP through targeting its promoter [15]. Therefore, *S. constricta* holds the potential to serve as a model organism to elucidate the intriguing mystery mentioned above.

In the present study, we first characterized the homologous gene of mammalian Ubxd8 from *S. constricta* (*Sc*Ubxd8) based on its genomic data [22]. Subsequently, we purified the protein encoded by *Sc*Ubxd8, namely *Sc*UBXD8, *in vitro* through prokaryotic expression and assessed its sensitivity to different types and concentrations of FA. Further, we examined the regulatory role of *Sc*UBXD8 in LC-PUFA biosynthesis in *S. constricta in vivo* through *Sc*Ubxd8 knockdown. These results confirmed the conserved function of UBXD8 in *S. constricta*, providing valuable insights into the regulation of LC-PUFA homeostasis and biosynthesis in marine mollusks, thereby contributing to the efficient utilization of their LC-PUFA resources.

2. Materials and methods

All animal experiments were carried out following the guidelines and with the approval of the Animal Research and Ethics Committees of Ningbo University.

2.1. Cloning of ScUbxd8

Using the human Ubxd8 sequence (NP_055428.1) as a reference, the homologous gene of *S. constricta* was identified from its genomic data [22]. To verify the sequence, the open reading frame (ORF) of *Sc*Ubxd8 was amplified through polymerase chain reaction (PCR). This was achieved using the Mighty Amp™ DNA polymerase version 3 (TaKaRa, Japan) and specific primers mentioned in Table 1. In detail, the total of RNA was firstly extracted from a mixture of *S. constricta* foot, intestine, and digestive glands using the Trizol method. Subsequently, 1 μg of RNA was reverse transcribed into cDNA utilizing the PrimeScript™ RT-PCR Kit (TaKaRa). The PCR reaction was carried out on a PCR instrument (Eppendorf, Germany) using the cDNA as the template. Following amplification, the resulting targeted PCR product was purified and inserted into pMD™ 18-T Vector (Takara). The vector containing the insert was then transformed into *Escherichia coli* DH5α competent cells. The positive single colonies on LB plates containing ampicillin (50 $\mu g \cdot mL^{-1}$) were selected, incubated, and subsequently subjected to sequencing conducted by Hangzhou Youkang Biotechnology Co., Ltd., China.

2.2. Sequence and phylogenetic analyses of ScUbxd8

To predict the potential functional domains, the deduced amino acids (aa) of *Sc*Ubxd8 was analyzed using the online SMART software (http://smart.embl-heidelberg.de/smart/set_mode.cgi?NORMAL=1). Meanwhile, the deduced aa of Ubxd8 from *S. constricta* and representative vertebrates, including *H. sapiens* (NP_055428.1), *M. musculus* (NP_848484.2), and *D. rerio* (AAI63084.1), were aligned using the ClustalW 2.1 software [26]. To uncover evolutionary relationships, the deduced aa sequences of Ubxd8 from *S. constricta*, representative vertebrates, and marine mollusks were analyzed using the Maximum-likelihood method in MEGA 7 software [27]. For root placement, an outgroup, the Ubxd8 homolog from *Saccharomyces cerevisiae* known as Ubxd2 (QHB10722.1) was selected [28]. The branch topology of the phylogenetic tree was bootstrapped with 1000 iterations.

2.3. Tissue expression of ScUbxd8

To identify the potential functional tissues of *Sc*Ubxd8, we collected various tissues from adult *S. constricta* individuals (55.03 ± 3.15 mm, shell length), including exhalent siphon, inhalant siphon, gill, labial palps, mantle, foot muscle, digestive glands, gonad, and intestine. These collected tissues were then employed for quantitative real-time PCR (qPCR). Each tissue sample was sourced from three individuals and prepared in quadruplicate. Firstly, total RNA was extracted from the collected tissues using the Trizol method. Then, 1 μg RNA was reverse transcribed into cDNA utilizing the PrimeScript™ RT Master Mix (Perfect Real Time, TaKaRa). The qPCR amplifications were performed on a quantitative thermal cycler (Mastercycler ep realplex, Eppendorf, Germany), using SYBR® Premix Ex Taq™ II (Tli RNaseH Plus) (TaKaRa) and specific primers (Table 1). The qPCR protocol was composed of an initial denaturation at 95 °C for 30 s, followed by 40 cycles of denaturation at 95 °C for 5 s and annealing and extension at 60 °C for 30 s, along with a melting curve analysis from 58 to 95 °C at an increment of 1.8 °C/min. The data was analyzed using the $2^{-\Delta\Delta CT}$ method [29] and normalized by the housekeeping gene β-actin (Table 1).

2.4. Prokaryotic expression and purification of ScUBXD8 and mutants

The recombinant prokaryotic vector was firstly constructed. In brief, the ORF of *Sc*Ubxd8 was cloned using the Mighty Amp™ DNA polymerase version 3 (TaKaRa) with specific primers harboring *Bam*HI and *Xho*I restriction sites (Table 1). Subsequently, the resulting PCR product was purified, digested with corresponding restriction endonucleases (New England Biolabs), and inserted into the pET-28a Vector (Novagen) that had been similarly digested. The insertion was performed using the DNA Ligation Kit Ver 2.1 (TaKaRa). The resulting recombinant vector was then transformed into *E. coli* Rosetta (DE3) competent cells. The positive single colonies were selected from LB plates containing

Table 1
Primers used in the present study. Primers with bases that are both bold and italic indicate the presence of restriction sites.

Aim	Primer	Sequence	Product (bp)
ORF cloning	*Sc*Ubxd8-F	ATGGCCGACGCAGCAGA	1341
	*Sc*Ubxd8-R	TCATGCTTCATTATCCTGAACAAAA	
	pET28a-*Sc*Ubxd8-F	CG***GAATTC***ATGGCCGACGCAGCAGA	1341
	pET28a-*Sc*Ubxd8-R	GG***GGTACC***TGCTTCATTATCCTGAACAAAAAGA	
	pET28a-*Sc*UAS-F	CG***GAATTC***GATGTTGAAAGATTTATTACCAACT	399
	pET28a-*Sc*UAS-R	GG***GGTACC***TTACATCACAGATTCTAGACGCT	
Plasmid construction	L4440-EGFP-F	TCC***CCGCGG***ATGGTGAGCAAGGGCGAG	720
	L4440-EGFP-R	CCG***CTCGAG***TTACTTGTACAGCTCGTCCATGC	
	L4440-*Sc*Ubxd8-F	CCC***AAGCTT***GGCACAGATCACCCTGTGTT	342
	L4440-*Sc*Ubxd8-R	CCG***CTCGAG***ACGCTGGATCAAGTCTCTTCC	
qPCR	q-*Sc*Ubxd8-F	AGACACTTCAGCGCCACAAT	125
	q-*Sc*Ubxd8-R	ATCCATTTGAGGGGCACGAG	
	q-Δ5 Fada-F	ACATCCCAGGCCCAAGGC	113
	q-Δ5 Fada-R	CCCTTGACAAACCCGGTCAA	
	q-Δ5 Fadb-F	TTATTCCACATCCCAGGTACAGACT	120
	q-Δ5 Fadb-R	CCCTTTGTGAAGCCCATGGT	
	q-Δ6 Fad-F	CTAACGAGGTGGACTTTGATGG	269
	q-Δ6 Fad-R	AGAGTGTTCCAAGGACCTGACC	
	q-Elovl2/5-F	GCTCAACATTTGGTGGTGGGT	120
	q-Elovl2/5-R	GGAATGACTGCCAGACCGTAG	
	q-Elovl4a-F	TTGGGATCATTCACGCAGCC	92
	q-Elovl4a-R	GATGGTGAATGCGTAAAACACAAGA	
	q-Elovl4b-F	TGCCGGTATGGTCTACGGTGT	94
	q-Elovl4b-R	GATTGTGACACCGTATACAAGCGAG	
	q-Elovlc-F	TGCTATCTACTCGGACTGTGGC	141
	q-Elovlc-R	GTTTTCTTGACGTGTGCAGAGC	
	q-Insig-F	TCACTACGAGTCCTCATGGTGG	119
	q-Insig-R	ACTCTCCCCTGTACTTGAATGGTT	
	q-Srebp-F	CTGGGTCAGAATGAACGGCTA	175
	q-Srebp-R	GAGAGTTGGGTGGCGAGACA	
	q-Fas-F	CTATGTCGAGGCCCATGGTACT	134
	q-Fas-R	CCGAGTGACCCATGTTCGAT	
	q-*β*-actin-F	CCATCTACGAAGGTTACGCCC	117
	q-*β*-actin-R	TCGTAGTGAAGGAGTAGCCTCTTTC	

ampicillin (50 μg·mL^{-1}) and chloromycetin (34 μg·mL^{-1}), followed by incubation and sequencing conducted by Hangzhou Youkang Biotechnology Co., Ltd., China.

The successfully recombinant cells were cultured in LB medium supplemented with ampicillin (50 μg·mL^{-1}) and chloramphenicol (34 μg·mL^{-1}) at 37 °C. Upon reaching the mid-logarithmic phage, isopropyl thiogalactoside (IPTG) was added to a final concentration of 0.4 mM to induce the expression of *Sc*UBXD8. Subsequently, the culture was further incubated at 16 °C for 12 h. The bacterial cells were then centrifuged at 8000 ×*g* at 4 °C for 10 min. The resulting cell pellet was dissolved in a binding buffer (20 mM Tris-base, 500 mM NaCl, pH 7.9), and subjected to ultrasonication. After achieving clarity, centrifugation (12,000 ×*g*, 4 °C, 30 min) was carried out, and the resulting supernatant was utilized for protein extraction using His60 Ni Gravity Columns (Clontech). The target protein was subsequently purified and eluted using varying concentrations of imidazole. It was then concentrated using an ultrafiltration centrifugal tube (Solarbio Science & Technology Co. Ltd., Beijing, China). The integrity of purified protein was confirmed through SDS-PAGE, while its concentration was determined using the Enhanced BCA Protein Assay Kit (Beyotime Biotech Co. Ltd., Shanghai, China).

Meanwhile, to confirm the critical domain responsible for FA sensing, proteins corresponding to the UAS domain (*Sc*UAS) and the domain lacking UAS (*Sc*DUAS) of *Sc*UBXD8 were obtained using similar methods as described above. Notably, the gene sequence of *Sc*DUAS was directly synthesized by Hangzhou Youkang Biotechnology Co., Ltd., China.

2.5. FA sensing analysis of purified proteins by blue native PAGE

Following the previously described method [19], the purified protein (1 μg) was firstly incubated with corresponding FA (NU-CHEK PREP, INC, USA) within an incubation buffer (25 mM Tris-HCl, 0.15 M NaCl, 1 mM DTT, PH 7.2) at 25 °C for 5 min (final volume, 18 μL). The included FA comprised saturated fatty acids (SFA) (16:0 and 18:0), monounsaturated fatty acids (MUFA) (12:1n-1, 14:1n-5, 16:1n-7, and 18:1n-9), and polyunsaturated fatty acids (PUFA) (LA, ALA, ARA, 20:4n-3, EPA, and DHA), added at final concentrations of 0, 1, 5, 10, 20, 50, 100, 200, 500, and 1000 μM, as indicated in the corresponding Figure legends. It's important to note that these FA were in their free form, dissolved in 100 % ethanol, and underwent no additional treatment, such as conjugation with defatted albumin. Subsequently, the mixture was supplemented with 2 μL of 10× loading buffer (5 mM Bis-Tris, 60 % Glycerol, 0.5 μg·mL^{-1} Coomassie G-250, 10 mg·mL^{-1} 6-Aminocaproic acid, PH 7.0), and subjected to Blue native PAGE analysis [30]. The blue native gel electrophoresis was performed using the NativePAGE™ 3–12 % Bis-Tris Gel (Invitrogen). The anode buffer consisted of 50 mM Bis-Tris (PH 7.0), while the cathode buffer was composed of 50 mM Tricine, 15 mM Bis-Tris, and 0.02 % Coomassie G-250 (m/v) (PH 7.0).

2.6. Knockdown of ScUbxd8 by ingesting dsRNA-expressing bacteria

RNA interference (RNAi) through the ingestion of dsRNA-expressing bacteria has been demonstrated as a relatively simple, cost-effective, non-invasive, and efficient method for knocking down functional genes in bivalves [31–33]. Based on this method, the full-length sequence of EGFP (used as a control) and a partial sequence of *Sc*Ubxd8 containing the UAS domain were firstly constructed into the L4440 vector (Huayueyang Biotechnology Co., Ltd., Beijing, China), respectively. This construction was accomplished using specific primers that harbored corresponding restriction sites (Table 1). The resulting recombinant plasmids, L4440-EGFP and L4440-*Sc*Ubxd8, were then individually transformed into *E. coli* HT115 (DE3) competent cells.

Subsequently, the positive single clones were cultured in LB medium supplemented with ampicillin (50 μg·mL^{-1}) and tetracycline (12.5 μg·mL^{-1}) at 37 °C until reaching an optical density of OD_{595} = 0.4. At this point, 0.4 mM IPTG was added to induce dsRNA expression, with the culture maintained at 37 °C for 4 h. The induced dsRNA was verified through RNA extraction using the Bacteria RNA Extraction Kit (Vazyme, China) and electrophoresis on a 1 % agarose gel.

The recombinant bacteria expressing dsRNA targeting EGFP (iEGFP) or *Sc*Ubxd8 (iUbxd8) were mixed with the microalgae *Platymonas subcordiformis* (100:1) and subsequently provided as feed to juvenile *S. constricta* (shell length, 2.11 ± 0.04 mm). The final concentration of *P. subcordiformis* for feeding was maintained at ~1 × 10^4 cells·mL^{-1}. The juvenile razor clams were reared in aquariums (dimensions: length × width × height = 20 × 20 × 20 cm), each containing a 1 cm layer of fresh sea mud and a 15 cm depth of filtered seawater (18 psu). Each treatment was replicated in triplicate, and every aquarium housed 100 individuals. The juveniles were fed with *P. subcordiformis* twice daily, at 10:00 am (mixed with bacteria expressing dsRNA) and 20:00 pm (without bacteria). The decision to feed the reared *S. constricta* only during the first feeding was primarily based on two reasons. Firstly, from our preliminary results, it appeared that providing bacteria expressing dsRNA solely during the first daily feeding efficiently knocked down the expression of *Sc*Ubxd8. Secondly, to maintain optimal water quality and prevent potential impacts on the ingestion and health of the reared *S. constricta*, we opted against continuously introducing bacteria expressing dsRNA throughout the entire culture period. Notably, approximately 2/3 of the seawater in the aquariums was renewed daily just before the second feeding. The experiment was conducted in a controlled environment at 20 °C, with a 12-h light cycle (8:00 am to 8:00 pm) followed by a 12-h dark cycle. Throughout the experiment, the knockdown efficiency of *Sc*Ubxd8 was assessed by qPCR as described earlier, involving the sampling of 10 individuals from each aquarium on the 7th, 14th and 28th d, respectively. At the end of the 28-d experiment, the juveniles were subjected to a one-day fasting period to facilitate digestion of ingested microalgae. Subsequently, the juveniles were collected, frozen in liquid nitrogen, and stored at −80 °C for further analyses.

2.7. Analysis of gene expression

The gene expression related to LC-PUFA biosynthesis in the collected *S. constricta* specimens was analyzed using qPCR, following the aforementioned procedure. The target genes included Fads (Δ5 Fada, Δ5 Fadb, and Δ6 Fad) [24] and Elovls (Elovl2/5, Elovl4a, Elovl4b, and Elovlc) [25]. Furthermore, the genes Fas (fatty acid synthase, the initial gene involved in LC-PUFA synthesis from Malonyl-CoA), Srebp [15], and Insig from *S. constricta* were also included in the qPCR analysis. It's worth noting that, similar to other invertebrates, *S. constricta* possesses only one homolog of Insig in its genome [22]. These specific qPCR primers were provided in Table 1.

2.8. Analysis of lipid content and FA composition

The lipid content of the collected *S. constricta* specimens was analyzed using the modified Blight and Dyer method [34]. Briefly, the crude lipid from 20 mg of freeze-dried *S. constricta* was extracted using $CHCl_3/CH_3OH/H_2O$ (1:2:0.8, v/v/v), with the addition of 0.01 % butylated hydroxytoluene (BHT) as an antioxidant. The extracted lipid was then dried under nitrogen until a constant weight was achieved, and the weight was recorded.

Based on the extracted lipid, the FA composition was further analyzed using our previously described method [35]. In brief, the crude lipid was redissolved in 0.2 mL of toluene, 1.5 mL of methanol, 0.3 mL of HCl (8 %, w/v) in methanol/water (85:15, v/v), and 15 μL of 19:0 (1 μg·μL^{-1}) as an internal standard (Cayman Chemicals, USA). The mixture was then incubated at 100 °C for 1 h to obtain FA methyl esters (FAME). The FAME was subsequently extracted using hexane-chloroform (4:1, v/v) containing 0.01 % BHT, dried under nitrogen, redissolved in 1 mL of chromatography-grade hexane, filtered through a 0.22 μm organic phase membrane, and analyzed using an Agilent GC–MS system (7890B/7000C).

The CD-2560 capillary column (100 m × 250 μm × 0.2 μm, CNW, Germany) was employed to separate the FAME. Helium was served as the carrier gas at a flow rate of 0.81 mL·min^{-1}. An injection volume of 1 μL was utilized in split-less mode. The GC oven temperature was maintained at 140 °C for 5 min, followed by a ramp to 240 °C over 20 min at a rate of 4 °C·min^{-1}. The injector temperature was set to 250 °C with an initial precolumn pressure of 30.36 psi. The MS ion source temperature was 230 °C, the transmission line temperature was 255 °C, and the quadrupole temperature was 150 °C. The collision energy was 70 ev. The MS scanning range was set from 40 to 600 *m/z*. FA identification was achieved by comparing characteristic fragments with the mass spectral database (NIST 14.L) and matching relative retention times with available commercial FA standards. The percentage composition (%) of each FA was determined by calculating the proportion of its area in the total FA area. Additionally, the content composition (μg·mg^{-1}) of each FA was calibrated using the area of the 19:0 standard (15 μg) and the weight of the lyophilized sample (20 mg).

Meanwhile, to assess the potential impact of dietary *P. subcordiformis* on *S. constricta*'s FA composition and LC-PUFA biosynthesis, the FA composition of *P. subcordiformis* was analyzed using the same method as mentioned above.

2.9. Statistical analysis

All data were presented as mean ± standard deviation (SD). For comparisons between two groups, the Student's *t*-test was used for statistical analysis (GraphPad, 8.0.2). For comparisons involving more than two groups, analysis of variance (ANOVA) followed by the Newman-Keuls test was utilized for statistical analysis (SPSS 22.0). Statistical significance was denoted by asterisks: * for P values <0.05, ** for P values <0.01, and *** for P values <0.001, or indicated by different letters to signify significant differences. Moreover, the amount of the unpolymerized *Sc*UBXD8 in Blue native PAGE was quantified using the ImageJ software v1.8.0.3.

3. Results

3.1. The sequence of ScUbxd8 is highly conserved during evolution

The ORF of *Sc*Ubxd8 gene spanned 1341 bp, encoding a protein consisting of 446 aa. The detailed sequence of *Sc*Ubxd8 has been deposited in the NCBI database under the accession number OR133611. The *Sc*UBXD8 protein exhibited all the typical characteristic domains of mammalian UBXD8 [19], including the UBA, UAS, and UBX domains (Fig. 1 A and B). Moreover, the critical positively charged aa that play a pivotal role in UBXD8 polymerization [19] were conserved in *Sc*UBXD8 (highlighted by asterisks [*] in Fig. 1B).

3.2. ScUbxd8 is phylogenetically conserved and highly expressed in digestive tissues

The phylogenetic analysis shown that *Sc*Ubxd8 clustered with homologs from other bivalves and further with those from gastropods such as *Lottia gigantea*, *Aplysia californica*, and *Biomphalaria glabrata* (Fig. 2A). In contrast, the vertebrate Ubxd8 formed a distinct cluster, encompassing both teleosts and mammals (Fig. 2A). This collective grouping was clearly further separated from the outgroup, which is represented by *S. cerevisiae* Ubxd2 [28].

The transcript of *Sc*Ubxd8 was detected in all the tissues examined (Fig. 2B). Remarkably, the highest expression of *Sc*Ubxd8 was observed in the intestine, followed by the digestive glands and labial palps. In

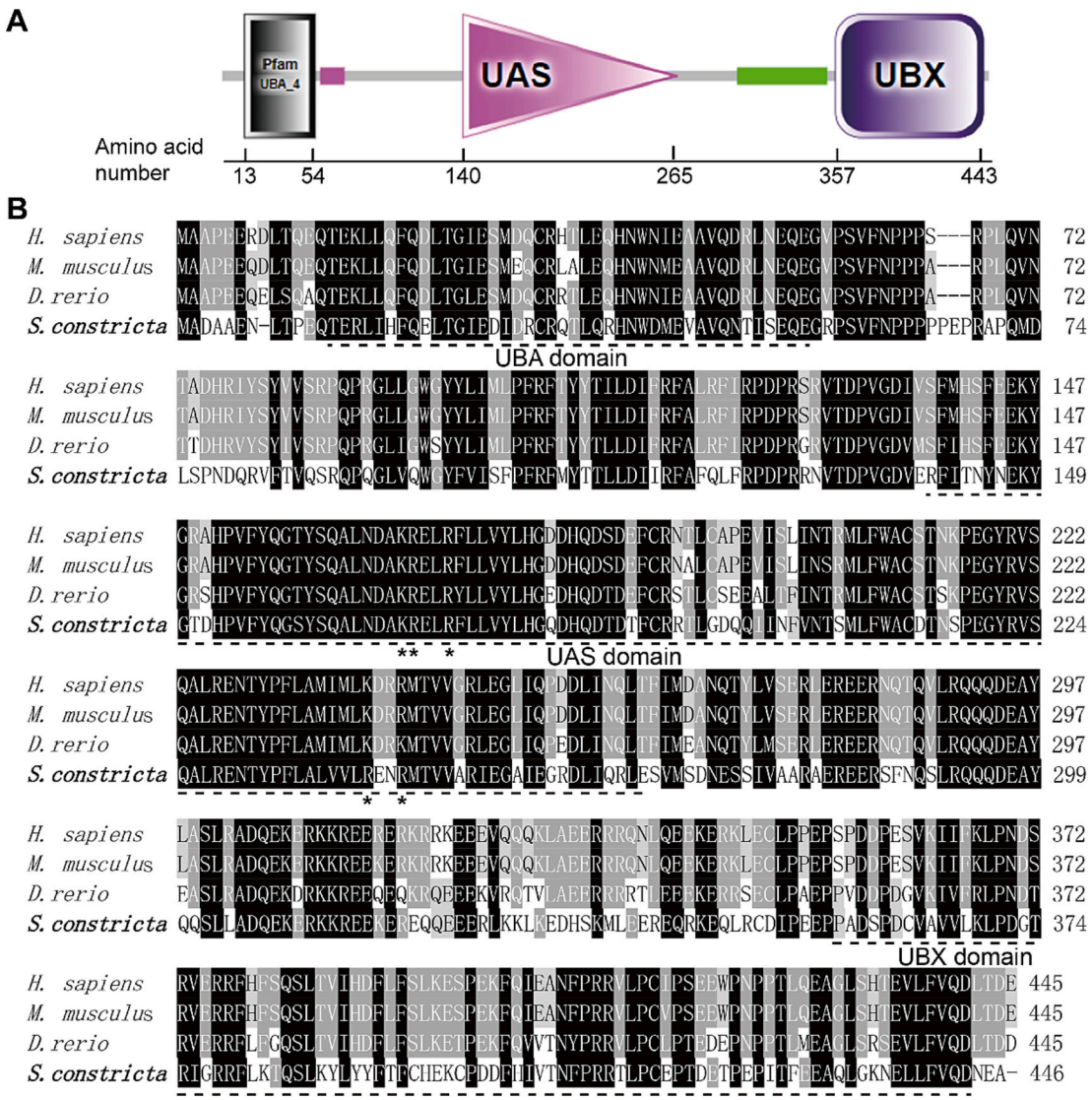

Fig. 1. Functional domain and aa sequence are conserved in *Sc*UBXD8. **A:** The functional domains of *Sc*UBXD8. The prediction was conducted by SMART software. **B:** The aa sequence alignment of *Sc*UBXD8. The alignment was compared with those from *H. sapiens* (NP_055428.1), *M. musculus* (NP_848484.2), and *D. rerio* (AAI63084.1) by ClustalX 1.83. The conserved domains of UBA, UAS, and UBX were highlighted with dashed lines. The positively charged aa residues involved in UBXD8 polymerization were highlighted with asterisks (*).

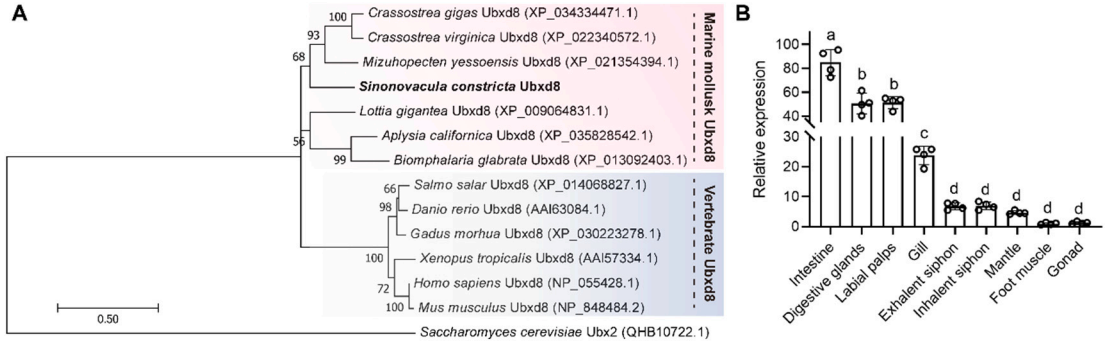

Fig. 2. *Sc*Ubxd8 is phylogenetically conservative and highly expressed in digestive tissues. **A:** The phylogenetic tree of *Sc*Ubxd8. The tree was constructed by comparing the deduced aa sequence of *Sc*Ubxd8 (bold) with orthologues from representative vertebrates and invertebrates. The tree was constructed using the Maximum Likelihood method based on the JTT matrix-based model of MEGA 7.0. The horizontal branch length is proportional to the aa substitution rate per site. The numerical values indicate the percentages of tree topology replication after 1000 iterations. **B:** The tissue distribution of *Sc*Ubxd8. The gene expression was analyzed by qPCR using the $2^{-\Delta\Delta CT}$ method. The values (mean ± SD, $n = 4$) sharing a common letter (a-d) above histograms were not significantly different ($P \leq 0.05$).

comparison, the gill exhibited relatively lower expression of *Sc*Ubxd8. Conversely, the expression of *Sc*Ubxd8 in other tissues was notably low, with no significant differences observed among them (Fig. 2B).

3.3. *ScUBXD8 functions in sensing LC-PUFA pool*

When the purified *Sc*UBXD8 protein (Fig. 3A) (1 μg) was incubated with corresponding FA (Fig. 3B) (200 μM), the results revealed distinct responses of *Sc*UBXD8 to different types of FA (Fig. 3C). This was evidenced in the polymerized forms (indicated by the broad band at the top of the gel) and the unpolymerized forms (indicated by the single band at the bottom of the gel) of *Sc*UBXD8 (Fig. 3C, left panel). Furthermore, the degree of *Sc*UBXD8 polymerization was assessed by quantifying the amount of unpolymerized *Sc*UBXD8 (Fig. 3C, right panel). Specifically, no polymerization of *Sc*UBXD8 was observed when incubated with SFA of 16:0 and 18:0 (Fig. 3C, lanes 2 and 3), mirroring the control condition (Fig. 3C, lane 1, no FA), resulting in a single band representing the unpolymerized *Sc*UBXD8. In contrast, incubation with UFA (16:1n-7, 18:1n-9, LA, ALA, ARA, EPA, and DHA) led to the polymerization of *Sc*UBXD8 (Fig. 3C, lanes 4–10), resulting in the appearance of a broad band of polymerized *Sc*UBXD8. Interestingly, the intensity of *Sc*UBXD8 polymerization progressively increased with higher unsaturation degrees and longer acyl chain lengths of UFA. Notably, for UFA located at the same node in the LC-PUFA biosynthetic pathway (Fig. 3B) [36], such as LA and ALA (Fig. 3C, lanes 6 and 8) or ARA and EPA (Fig. 3C, lanes 7 and 9), *Sc*UBXD8 exhibited a more pronounced sensitivity to n-6 UFA compared to n-3 UFA. This sensitivity was indicated by the amount of unpolymerized *Sc*UBXD8 (Fig. 3C).

To investigate whether the polymerization is dependent on FA concentration, we conducted incubations of *Sc*UBXD8 (1 μg) with varying levels (0, 1, 5, 10, 20, 50, 100, 200, 500, and 1000 μM) of specific FA (Fig. 4). The results, as depicted in Fig. 4A–G, indicated a gradual increase in *Sc*UBXD8 polymerization with the rising concentrations of corresponding UFA. Notably, the UFA with longer acyl chains and greater unsaturation degrees required lower concentrations to induce *Sc*UBXD8 polymerization. Moreover, similar with the findings in Fig. 3C, the concentration of n-6 UFA (Fig. 4C and E) necessary for *Sc*UBXD8 polymerization was relatively lower compared to that of n-3 UFA (Fig. 4D and F), both of which occupied the same node in the LC-PUFA biosynthetic pathway [36]. Additionally, the band of the polymerized *Sc*UBXD8 broadened with increasing concentrations of corresponding UFA. However, it's important to note that even at an extremely high concentration of 1000 μM, no polymerization of *Sc*UBXD8 was detected when incubated with the SFA (Fig. 4H). Collectively, in general, for a given 1 μg of *Sc*UBXD8, the concentration required for its nearly complete polymerization induced by 16:1n-7 and 18:1n-9 exceeded 200 μM. Conversely, polymerization induced by LA and ARA occurred at concentration below 100 μM but above 50 μM, while that by ALA and EPA required over 100 μM but <200 μM. Lastly, DHA-induced polymerization occurred at approximately 50 μM.

Moreover, to explore whether the polymerization is influenced by the *Sc*UBXD8 content, we took DHA (100 μM) as an example and incubated it with varying amount (1, 3, and 5 μg) of *Sc*UBXD8 protein. As shown in Fig. 5 (left panel), the 100 μM DHA induced almost complete polymerization of 1 μg *Sc*UBXD8 (lane 2), but not 3 μg *Sc*UBXD8 (lane 3), and further obvious polymerization was not observed for 5 μg *Sc*UBXD8 (lane 4). This was evidenced by the quantified amount of unpolymerized *Sc*UBXD8 (Fig. 5, right panel).

Furthermore, to figure out whether UFA with shorter acyl chains than C16 can induce the polymerization, we selected 12:1n-1 and 14:1n-5 to incubate with *Sc*UBXD8. As depicted in Fig. 6A, the polymerization of *Sc*UBXD8 was virtually negligible when incubated with 12:1n-1, even

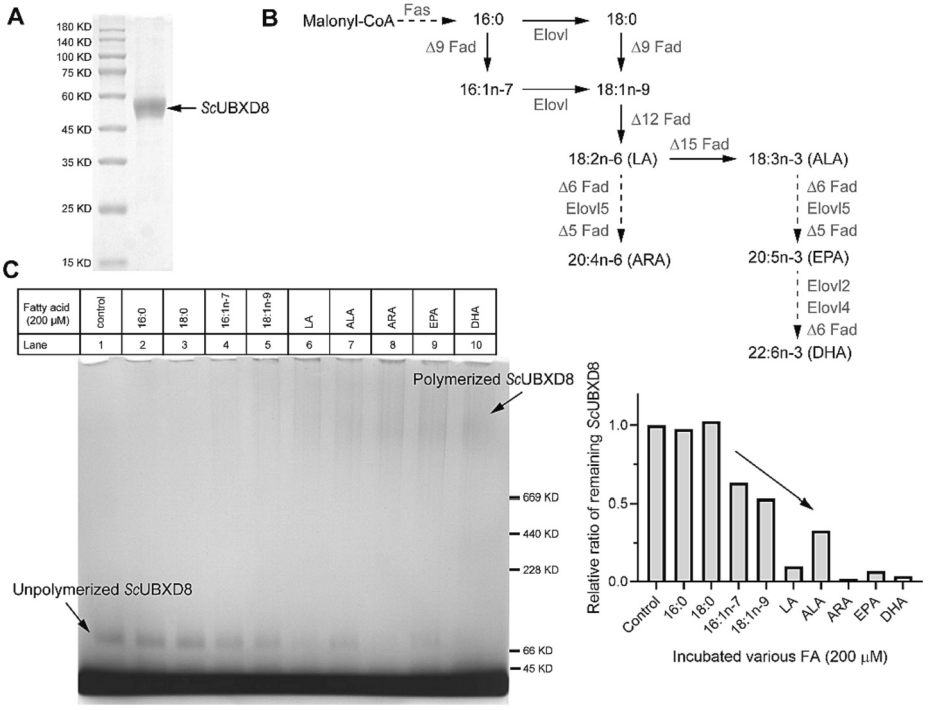

Fig. 3. *Sc*UBXD8 exhibits variable responses to different FA as evidenced by polymerization detection. **A:** The purified *Sc*UBXD8 protein. The *Sc*UBXD8 was purified by exogenously expression in *E. coli* Rosetta (DE3) cells. **B:** The distribution of selected FA in the LC-PUFA biosynthetic pathway. The catalytic enzymes were indicated by the grey fonts. **C:** The incubation of *Sc*UBXD8 (1 μg) with various FA (200 μM). The polymerized *Sc*UBXD8 was indicated by a broad band on the top of the gel, while the unpolymerized *Sc*UBXD8 was denoted by a single band at the bottom of the gel. Meanwhile, the relative ratio of unpolymerized *Sc*UBXD8 was quantified using the ImageJ software through normalizing to the control (no FA). The obvious decrease of the unpolymerized *Sc*UBXD8 was indicated by an arrow. Notably, the protein marker (PL00001, 10–180 KD) in Fig. 3A was obtained from Proteintech Group, Inc., USA. Additionally, the protein marker shown in Fig. 3C, High Molecular Weight Non-Denatured Protein Marker II (RTD6142, 45-669 KD), was sourced from Zhongke Ruitai (Beijing) Biotechnology Co., Ltd., China. Specific bands can be referenced in Fig. 4H.

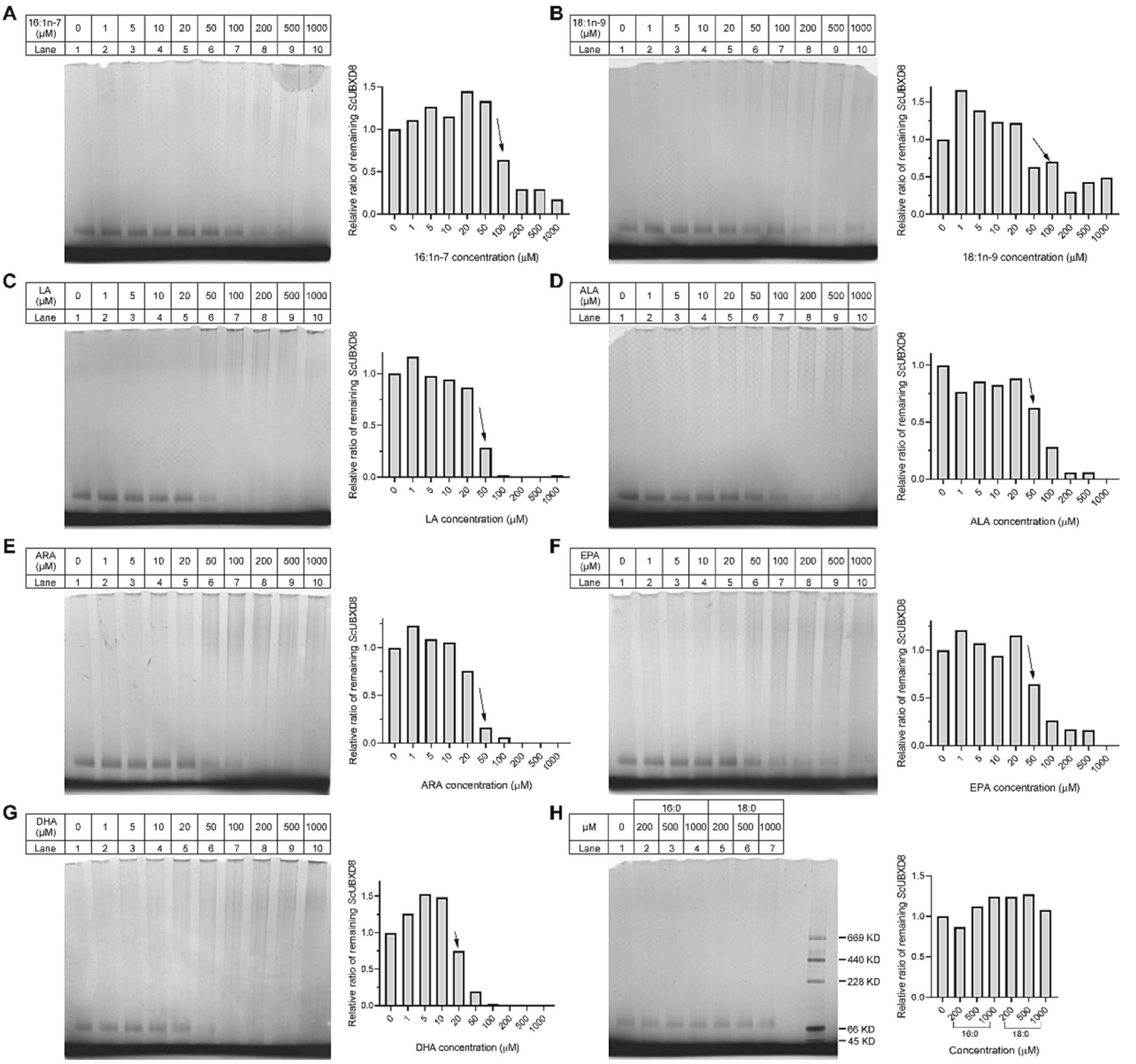

Fig. 4. Intensity of *Sc*UBXD8 polymerization is dependent on the concentration of FA. A–H: The incubation of *Sc*UBXD8 (1 μg) with various FA at different concentrations. The FA used for incubation included 16:1n-7 (A), 18:1n-9 (B), LA (C), ALA (D), ARA (E), EPA (F), DHA (G), 16:0 and 18:0 (H). The concentration was set at 0 (control), 1, 5, 10, 20, 50, 100, 200, 500, and 1000 μM. The other information was referred to Fig. 3C.

at a concentration of 1000 μM. In contrast, the polymerization of *Sc*UBXD8 was still detectable when incubated with a high concentration (≥200 μM) of 14:1n-5 (Fig. 6B).

To further clarify whether the positioning of double bonds in UFA influences the polymerization, we selected ARA (referring to Fig. 4E) and 20:4n-3 to incubate with *Sc*UBXD8. As exhibited in Figs. 4E and 6C, there were no apparent differences in the polymerization of *Sc*UBXD8 when incubated with ARA and 20:4n-3, at least for the present FA concentrations.

Lastly, to confirm whether the conserved UAS domain plays a crucial role in *Sc*UBXD8 polymerization as that reported in mammalian UBXD8 [19], we incubated the proteins *Sc*UAS (representing the UAS domain of *Sc*UBXD8) and *Sc*DUAS (which lacks the UAS domain of *Sc*UBXD8) (Fig. 7A) (1 μg) with various FA (200 μM), respectively. As illustrated in Fig. 7B, *Sc*UAS efficiently interacted with UFA, leading to substantial polymerization. In contrast, although some degree of polymerization was observed with *Sc*DUAS when incubated with UFA (Fig. 7C), the intensity significantly decreased compared to that of the native *Sc*UBXD8 (Fig. 3C).

3.4. *ScUBXD8 plays a regulatory role in LC-PUFA biosynthesis*

By ingesting the dsRNA targeting EGFP (control, iEGFP) or *Sc*Ubxd8 (iUbxd8) expressed in *E. coli* HT115 (Fig. 8A), the transcript of *Sc*Ubxd8 in juvenile *S. constricta* was significantly downregulated throughout the experiment (Fig. 8B). However, no significant differences were observed in shell length (Fig. 8C) and lipid content (Fig. 8D) between the iUbxd8 and iEGFP groups, despite an increasing trend in the iUbxd8 group. Conversely, the expression of genes related to LC-PUFA biosynthesis differed significantly between those two groups (Fig. 8E). Specifically,

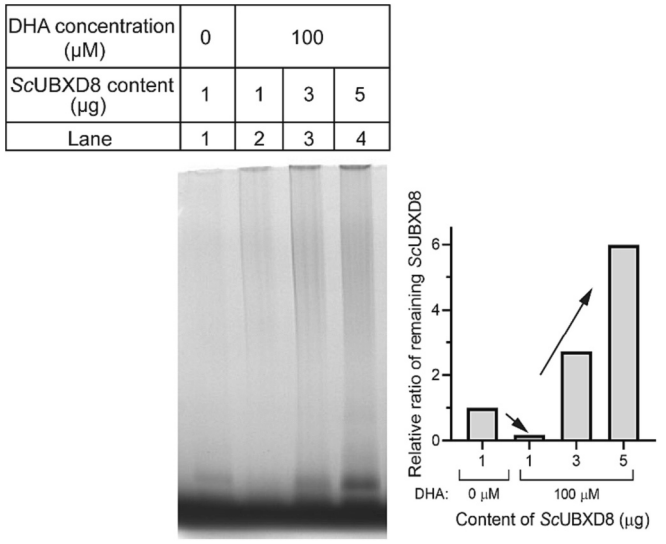

Fig. 5. A specific concentration of UFA corresponds to induction of a certain amount of *Sc*UBXD8 to polymerize. Using the DHA as an example, the 100 μM DHA was incubated with *Sc*UBXD8 at different contents (1, 3, 5 μg). The other information was referred to Fig. 3C.

compared with the control group, the expression of Δ5 Fada and Δ5 Fadb significantly increased upon *Sc*Ubxd8 knockdown, whereas that of Δ6 Fad, Elovl4a, Elovl4b, and Elovlc significantly decreased. Additionally, though Elovl2/5 expression did not show a significant difference ($P = 0.06$), it exhibited an increasing trend in the iUbxd8 group. In contrast, a decreasing trend in Fas expression was observed during *Sc*Ubxd8 knockdown, despite no significant difference observed ($P = 0.07$). Furthermore, the expression of Srebp increased significantly upon *Sc*Ubxd8 inhibition, while the expression of Insig decreased significantly.

To further confirm the regulatory role of *Sc*UBXD8 in LC-PUFA biosynthesis, we analyzed changes in the FA composition (%) of juvenile *S. constricta* when *Sc*Ubxd8 was knock down (Fig. 9 and Table S1). In comparison to the control group, in terms of SFA (Fig. 9A), the percentages of 15:0 and 16:0 increased significantly upon *Sc*Ubxd8 inhibition, while there were no significant differences in other SFA. When it comes to MUFA (Fig. 9B), the percentages of 18:1n-9 and 20:1n-7 decreased significantly with *Sc*Ubxd8 inhibition, but no significant differences were observed in other MUFA. As for PUFA (Fig. 9C), the percentages of ALA, 20:3n-6, and 22:3 [5,11,14] decreased significantly, while the percentages of EPA, 22:2 [5,13], 22:5n-6, 22:5n-3, and DHA increased significantly upon *Sc*Ubxd8 inhibition. Meanwhile, no significant differences were noted for other PUFA. Moreover, apart from SFA, whose total percentage was significantly higher in the iUbxd8 group compared to the control (Fig. 9D), there were no significant differences in the total percentage of MUFA and PUFA.

Furthermore, we analyzed changes in the content composition ($\mu g \cdot mg^{-1}$) of FA upon *Sc*Ubxd8 inhibition. As shown in Table S1, when *Sc*Ubxd8 was knock down, the contents of most of FA exhibited no significant differences compared to the control. Exceptionally, the content of ALA significantly decreased, whereas the contents of 15:0, 22:2 [5,13], EPA, and DHA increased significantly in comparison to the control.

4. Discussion

Marine mollusks serve as excellent sources of LC-PUFA for fulfilling human nutritional requirements [1]. Besides directly absorbing LC-PUFA from diets [14,37], such as microalgae rich in these FA [38], marine mollusks have demonstrated the capabilities to biosynthesize LC-PUFA endogenously [3]. As a result, the mechanism by which marine mollusks sense the levels and compositions of ingested FA to regulate their endogenous LC-PUFA biosynthesis remains an intriguing mystery to be elucidated. In this study, we presented UBXD8 as a critical and promising molecule involved in this enigmatic process.

The *Sc*UBXD8 contained all typical features found in mammalian UBXD8 (Fig. 1) [19], indicating the conserved function of UBXD8 throughout evolution. Furthermore, our investigation revealed that UBXD8 homologs are widespread among aquatic animals, including

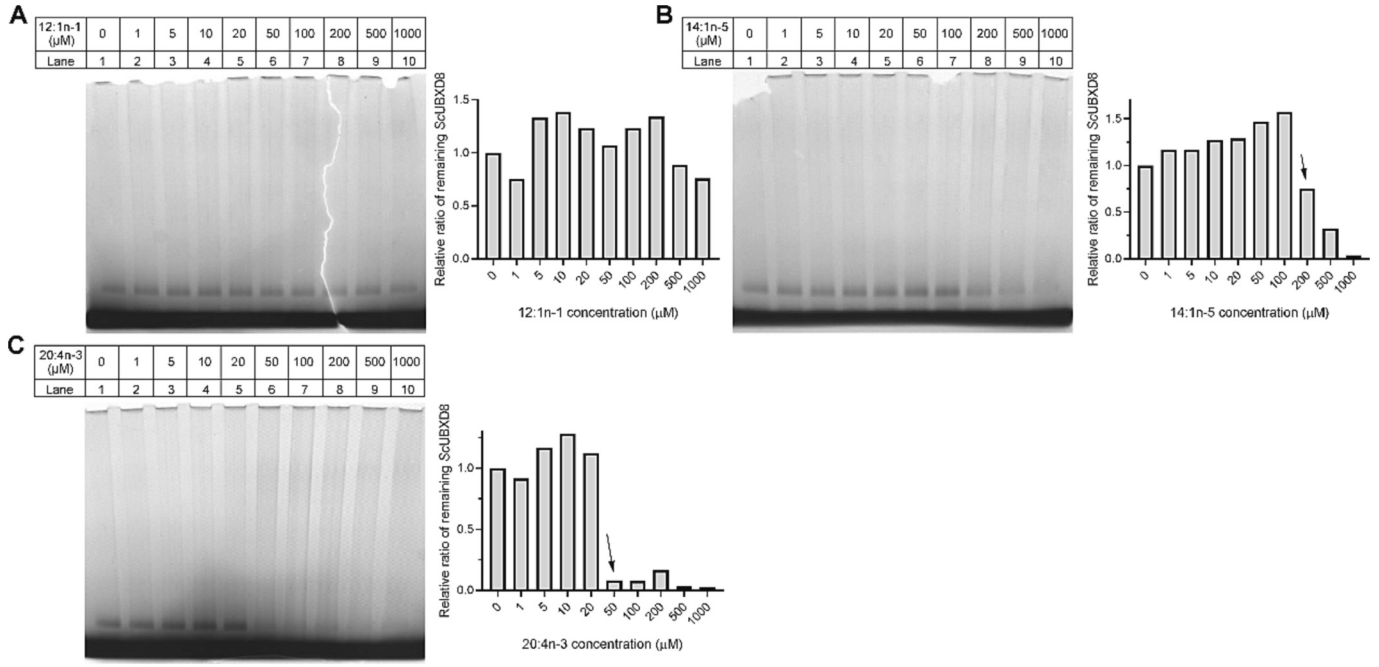

Fig. 6. Polymerization of *Sc*UBXD8 requires acyl chain length of UFA at least ≥ 14 but appears to be insensitive to the position of double bonds. **A** and **B:** The incubation of *Sc*UBXD8 (1 μg) with shorter UFA at different concentrations. These FA included 12:1n-1 (A) and 14:1n-5 (B). **C:** The incubation of *Sc*UBXD8 (1 μg) with 20:4n-3 at different concentrations. The other information was referred to Fig. 4.

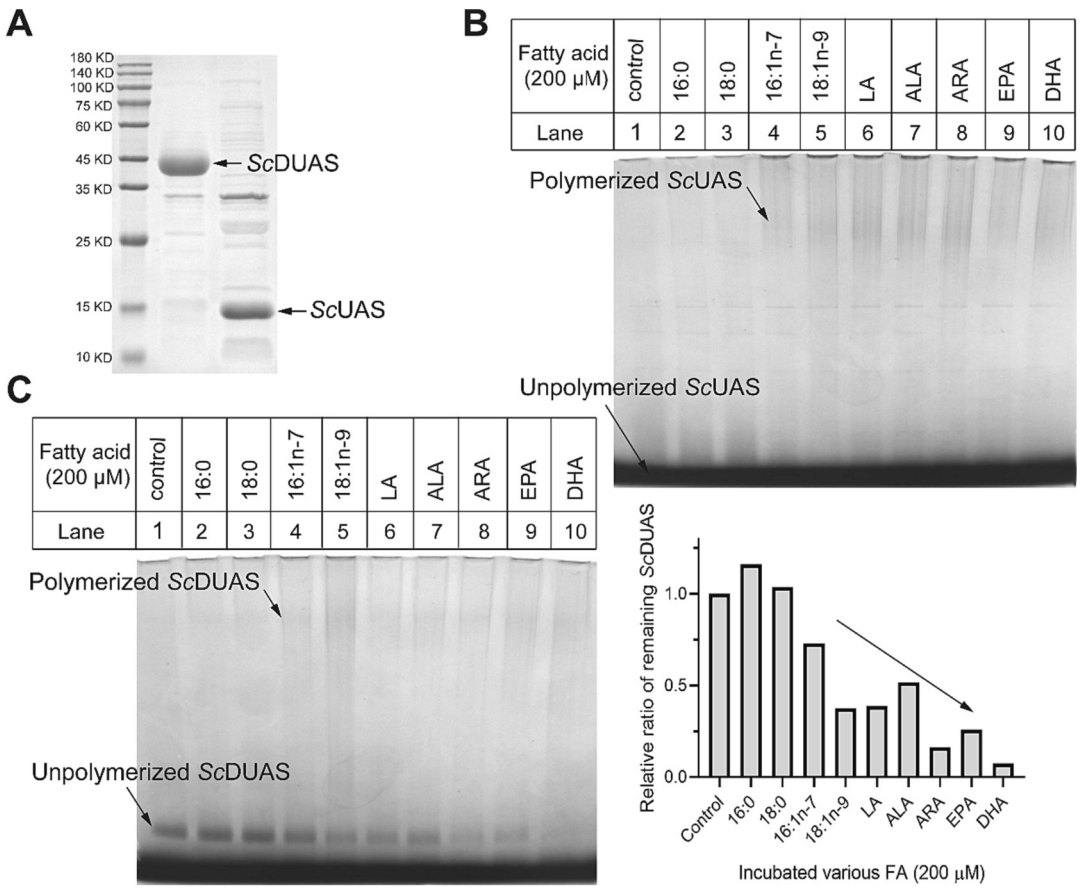

Fig. 7. UAS domain is essential for the efficient polymerization of *Sc*UBXD8. **A:** The purified protein of *Sc*UAS (UAS domain of *Sc*UBXD8) and *Sc*DUAS (*Sc*UBXD8 without UAS domain). Those proteins were purified by exogenously expression in *E. coli* Rosetta (DE3) cells. **B** and **C:** The incubation of *Sc*UAS (B) or *Sc*DUAS (C) (1 μg) with various FA at 200 μM. The other information was referred to Fig. 3C. Notably, the quantification of the unpolymerized *Sc*UAS in Fig. 7B was not feasible due to its coverage by the bottom lane of Coomassie G-250.

marine mollusks and teleosts (Fig. 2A), suggesting the conserved evolution of UBXD8 across animal species. Notably, the expression of *Sc*Ubxd8 was significantly higher in digestive tissues (intestine, digestive glands, and labial palps) compared to other tissues (Fig. 2B). This pattern of expression aligned with those of *S. constricta* Fads and Elovls [24,25], suggesting that *Sc*UBXD8 likely plays a regulatory role of in LC-PUFA biosynthesis within this bivalve.

While UBXD8 has long been recognized as an UFA sensor in mammalian cells [17], a comprehensive understanding of its sensitivity to different FA has remained incomplete [17,19]. In this study, we conducted a more systematic analysis of its UFA sensing role, focusing on *Sc*UBXD8. Consistent with the mammalian UBXD8 [17], the polymerization of *Sc*UBXD8 was triggered by UFA but not SFA (Fig. 3). Furthermore, the intensity of *Sc*UBXD8 polymerization gradually increased with acyl chain length, degree of unsaturation, and UFA concentration (Fig. 4). Exceptionally, *Sc*UBXD8 exhibited a more pronounced sensitivity to n-6 UFA compared to n-3 UFA (Fig. 4C–F), which are distributed in the same nodes in the LC-PUFA biosynthetic pathway [36]. These findings suggested that *Sc*UBXD8 might play a critical role in balancing the FA composition and the ratio of n-6/n-3 UFA in *S. constricta*. Consequently, we inferred that *S. constricta* may possess a preference for accumulating n-3 UFA over n-6 UFA, which could be a reason for the abundant presence of n-3 UFA in marine mollusks [1].

Additionally, we observed that the interaction between *Sc*UBXD8 and UFA was saturable and not unrestricted (Figs. 4 and 5). This suggested that artificially up or down-regulating *Sc*UBXD8 might offer a feasible approach for controlling the homeostasis and accumulation of UFA in *S. constricta*. Furthermore, our findings indicated that *Sc*UBXD8 polymerization required the acyl chain length of UFA at least ≥14 (Fig. 6A and B). Interestingly, *Sc*UBXD8 seemed to exhibit no sensitivity to the position of double bonds in UFA (Figs. 4E and 6C), although further investigations on more detailed concentrations of UFA are highly recommended. Moreover, the UAS domain was also found to be essential for the efficient polymerization of *Sc*UBXD8 (Fig. 7B), as reported in mammalian UBXD8 [19]. While the somewhat degree of *Sc*DUAS polymerization (Fig. 7C) might result from its unique dimensional structure. Collectively, those results provided further insights into the characteristics of *Sc*UBXD8 in UFA sensing.

It has been reported that knocking down Ubxd8 inhibits LC-PUFA biosynthesis in mammal cells [17]. This inhibition is attributed to the downregulation of UBXD8, which stabilizes INSIG1 and consequently prevents SREBP maturation [18]. To investigate whether a similar role exists for *Sc*UBXD8, we performed knockdown experiments targeting *Sc*Ubxd8 in juvenile *S. constricta* using dsRNA interference (Fig. 8A and B). As anticipated, inhibiting *Sc*Ubxd8 resulted in a significant decrease in the expression of several genes related with LC-PUFA biosynthesis, including Δ6 Fad, Elovl4a, Elovl4b, and Elovlc. However, the inhibition of *Sc*Ubxd8 also led to a remarkable increase in the expression of Δ5 Fada, Δ5 Fadb, and Elovl2/5 (although not statistically significant). This could be a compensatory response to the significant downregulation of Δ6 Fad expression, given that Δ6 Fad is upstream of Δ5 Fad and Elovl2/5 in the LC-PUFA biosynthetic pathway [36]. Meanwhile, Fas, a well-known target of matured SREBP, also displayed a decreasing trend, potentially attributed to the reduced maturation of SREBP. Similarly, the notable increase in Srebp expression might result from the inhibition of SREBP maturation upon *Sc*UBXD8 knockdown, while the significant

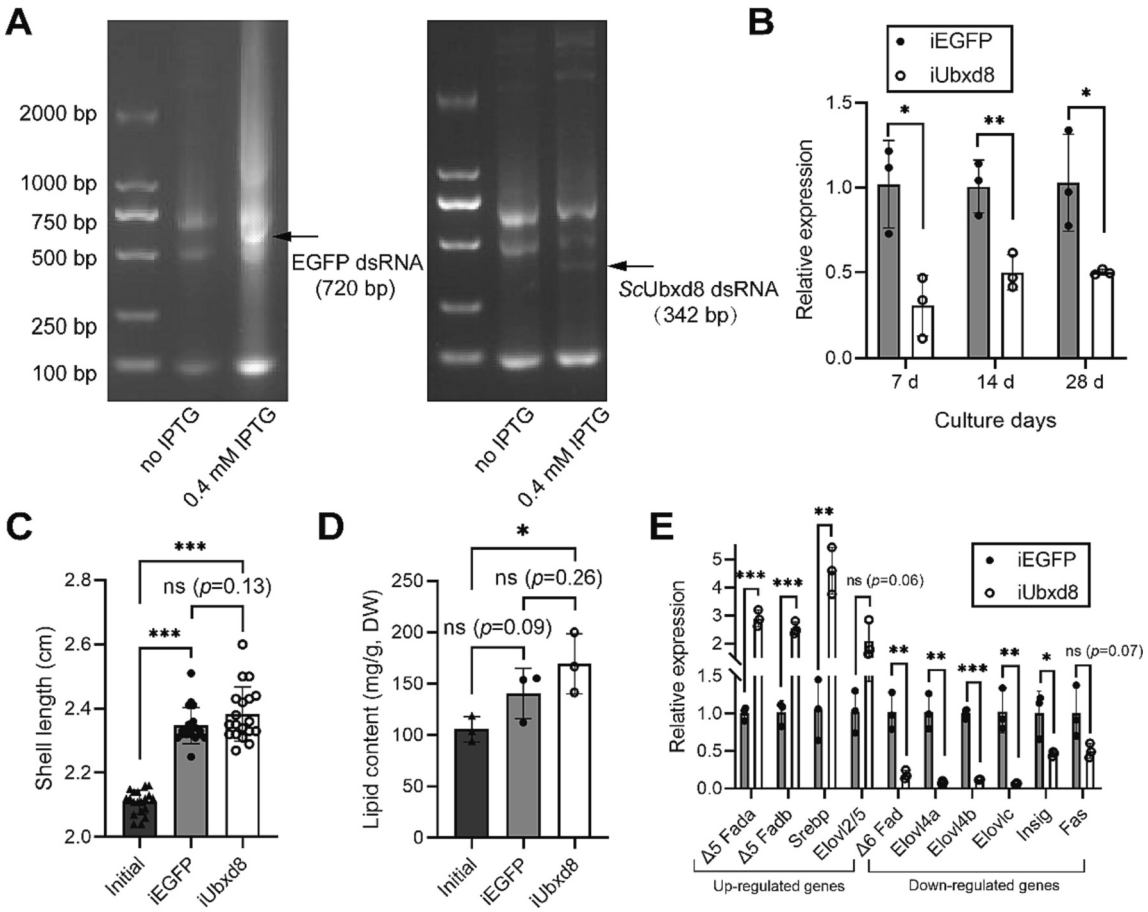

Fig. 8. Knockdown of *Sc*Ubxd8 disrupts lipid metabolism in *S. constricta*. **A:** The dsRNA expressed in *E. coli* HT115 (DE3). These dsRNA targeted either EGFP (control, iEGFP) or *Sc*Ubxd8 (iUbxd8). **B:** The inhibition of *Sc*Ubxd8 expression. The expression level of *Sc*Ubxd8 was detected by qPCR in juvenile *S. constricta* when fed with *E. coli* HT115 (DE3) expressing dsRNA. **C**–**E:** The effects of *Sc*Ubxd8 knockdown on growth (shell length) (C), lipid content (D), and expression of genes related to LC-PUFA biosynthesis (E) in *S. constricta*. The statistical significance was indicated by the * ($p < 0.05$), ** ($p < 0.01$), and *** ($p < 0.001$), respectively. While ns represented no statistical significance.

decrease in Insig expression could be a response to the stabilized INSIG. Honestly, a major limitation of our study was the unavailability of specific antibodies, which unfortunately hindered us from conducting the western blot assays to detect alterations in the protein levels of UBXD8, SREBP, and INSIG in *S. constricta* when *Sc*Ubxd8 was knock down. Nevertheless, the present results compelling indicated that knocking down *Sc*Ubxd8 would significantly disrupt LC-PUFA biosynthesis in *S. constricta*.

The regulatory role of *Sc*UBXD8 in LC-PUFA biosynthesis was further supported by changes observed in the FA composition upon *Sc*Ubxd8 inhibition (Fig. 9). Specifically, the percentages of shorter UFA, such as 18:1n-9, 20:1n-7, ALA, and 20:3n-6, experienced significant decreases. These changes might result from the inhibition of LC-PUFA biosynthesis due to the prevention of SREBP maturation, as discussed earlier. Consistently, the percentage of the initial LC-PUFA precursor, 16:0, was notably higher in the *Sc*Ubxd8 knockdown group. In contrast, the percentages of longer UFA, such as EPA, 22:5n-3, and DHA, showed significant increases. This finding was consistent with a previous study where the knockdown of Ubxd8 specifically promoted UFA accumulation as triglycerides in mammal cells [17]. Furthermore, this consistency was reinforced by the discovery that the contents of EPA, 22:2 [5,13], and DHA significantly increased upon *Sc*Ubxd8 inhibition (Table S1). This suggested that these FA might be stored, possibly as triglycerides, for future use when needed. This trend was also reflected in the increased lipid content (though not statistically significant) observed when *Sc*Ubxd8 was knockdown (Fig. 8D). Simultaneously, when knocking down *Sc*Ubxd8, we observed an increasing growth trend in juvenile *S. constricta* (Fig. 8C). This growth trend could possibly be attributed to the redirection of energy towards growth due to the inhibition of LC-PUFA biosynthesis. Taken together, though somewhat imaginative, we proposed that the downregulation of *Sc*Ubxd8 might create an analogous effect in *S. constricta*, akin to the inactivation achieved through polymerization of *Sc*UBXD8. This effect could give rise to a false impression of heightened of UFA in the body, subsequently suppressing LC-PUFA biosynthesis and promoting accumulation of these FA into triglycerides. Naturally, this hypothesis required further empirical validation.

Notably, it's indeed widely believed that LC-PUFA biosynthesis in marine mollusks like *S. constricta* is limited due to the ample availability of LC-PUFA in their diets, such as microalgae [3,38]. However, the retention of the complete LC-PUFA biosynthetic pathway in *S. constricta* highlights the critical nature of this ability when dietary LC-PUFA is insufficient or unavailable [24,25]. Our previous study demonstrated that *S. constricta* can extensively biosynthesize LC-PUFA by significantly modulating Fad and Elovl expression [39]. In the current study, despite *Sc*Ubxd8 knockdown, we did not observe marked changes in *S. constricta*'s FA composition (Fig. 9, Table S1). This lack of change might be attributed to the specific levels of certain LC-PUFA, such as ARA and EPA, present in the diet of *P. subcordiformis* (Table S1). These dietary components could potentially meet the LC-PUFA requirements of *S. constricta* to a considerable extent, possibly diminishing the significance of its endogenous LC-PUFA biosynthesis. Moreover, the role of *Sc*UBXD8 might be more critical for *S. constricta* when facing a diet frequently rich in LC-PUFA, aiming to prevent lipotoxicity by facilitating

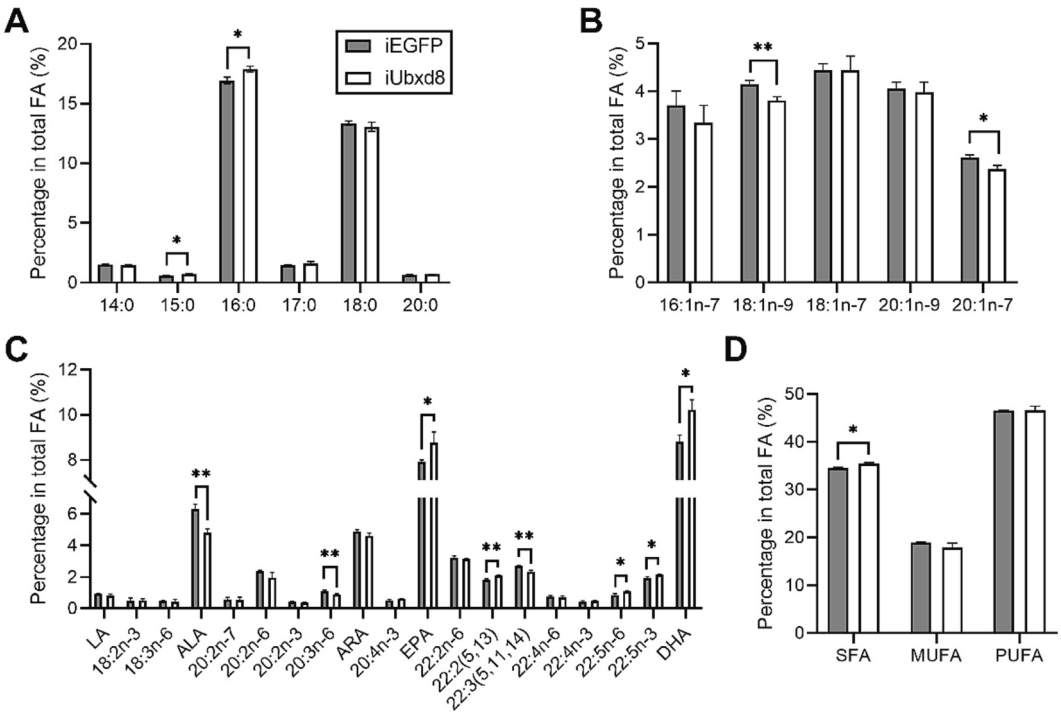

Fig. 9. Knockdown of *Sc*Ubxd8 alters FA composition in juvenile *S. constricta*. **A**–**D**: The changes of percentage composition of SFA (A), MUFA (B), PUFA (C), and their overall proportions (D). The statistical significance was indicated by the * ($p < 0.05$) and ** ($0.001 < p < 0.01$), respectively. While the absence of * indicated no statistical significance.

their storage as triglycerides within lipid droplets [17]. Our study consistently revealed that *Sc*Ubxd8 knockdown resulted in elevated levels of EPA and DHA (Fig. 9C). Collectively, these findings suggest that *Sc*UBXD8 should play a pivotal role in controlling the amount of LC-PUFA in *S. constricta*, not only by regulating endogenous LC-PUFA biosynthesis but also by storing excessive exogenous dietary LC-PUFA.

Furthermore, our analysis revealed a correlation between specific FA in *S. constricta* and those present in the diet of *P. subcordiformis* (Table S1). Notably, FA like 16:0, 16:1n-9, 18:1n-9, 18:1n-7, and ALA exhibited alignment, while others such as 16:3n-6, 16:4n-3, and LA did not follow the same pattern (Table S1). Meanwhile, despite the absence of C $\geq$ 20 LC-PUFA, except for low levels of ARA, 20:4n-3, and EPA in *P. subcordiformis*, FA like 22:3 [5,11,14] and DHA remained abundant in cultured *S. constricta* (Table S1). These findings highlight the selective accumulation of FA and the robust biosynthetic capacity of LC-PUFA by *S. constricta*, aligning with our previous discoveries [39].

In conclusion, this study provided the first molecular and functional evidence for LC-PUFA sensing and regulation in marine mollusks. The findings confirmed *Sc*UBXD8 as a sensor for UFA and a regulator in LC-PUFA biosynthesis in *S. constricta*. The results suggested that *S. constricta* might sense LC-PUFA pool through UBXD8 to keep homeostasis by regulating expression of genes associated with LC-PUFA biosynthesis, possibly *via* the INSIG-SREBP pathway. Collectively, our findings would be beneficial for future investigations on optimizing the LC-PUFA composition and accumulation in marine mollusks to meet human nutritional requirements.

Supplementary data to this article can be found online at https://doi.org/10.1016/j.bbalip.2023.159448.

CRediT authorship contribution statement

Zhaoshou Ran: Conceptualization, Formal analysis, Funding acquisition, Investigation, Methodology, Writing – original draft. **Haixuan Xie:** Data curation, Formal analysis, Investigation, Writing – review & editing. **Xuxu Tian:** Data curation, Formal analysis, Investigation, Writing – review & editing. **Fei Kong:** Data curation, Formal analysis, Investigation, Writing – review & editing. **Kai Liao:** Validation, Writing – review & editing. **Xiaojun Yan:** Validation, Writing – review & editing. **Jilin Xu:** Funding acquisition, Supervision, Writing – review & editing.

Declaration of competing interest

The authors have no conflict of interest to declare.

Data availability

Data will be made available on request.

Acknowledgements

This research was supported by the National Natural Science Foundation of China (32102763), the CSC scholarship funded by China Scholarship Council (202208330129), the Ningbo Science and Technology Research Projects, China (2019B10006), and the earmarked fund for CARS-49.

References

[1] K. Tan, H.K. Zhang, S.K. Li, H.Y. Ma, H.P. Zheng, Lipid nutritional quality of marine and freshwater bivalves and their aquaculture potential, Crit. Rev. Food Sci. 62 (2022) 6990–7014.
[2] I. Djuricic, P.C. Calder, Polyunsaturated fatty acids and metabolic health: novel insights, Curr. Opin. Clin. Nutr. Metab. Care 25 (2022) 436–442.
[3] Ó. Monroig, A.C. Shu-Chien, N. Kabeya, D.R. Tocher, L.F.C. Castro, Desaturases and elongases involved in long-chain polyunsaturated fatty acid biosynthesis in aquatic animals: from genes to functions, Prog. Lipid Res. 101157 (2022).
[4] Ó. Monroig, D. Guinot, F. Hontoria, D.R. Tocher, J.C. Navarro, Biosynthesis of essential fatty acids in *Octopus vulgaris* (Cuvier, 1797): molecular cloning, functional characterisation and tissue distribution of a fatty acyl elongase, Aquaculture 360-361 (2012) 45–53.
[5] Ó. Monroig, J.C. Navarro, J.R. Dick, F. Alemany, D.R. Tocher, Identification of a Δ5-like fatty acyl desaturase from the cephalopod *Octopus vulgaris* (Cuvier 1797)

involved in the biosynthesis of essential fatty acids, Marine Biotechnol. 14 (2012) 411–422.
[6] Ó. Monroig, R. De Llanos, I. VarÓ, F. Hontoria, D.R. Tocher, S. Puig, J.C. Navarro, Biosynthesis of polyunsaturated fatty acids in *Octopus vulgaris*: molecular cloning and functional characterisation of a stearoyl-CoA desaturase and an elongation of very long-chain fatty acid 4 protein, Mar. Drugs 15 (2017) 82.
[7] D. Garrido, N. Kabeya, F. Hontoria, J.C. Navarro, D.B. Reis, M.V. Martín, C. Rodríguez, E. Almansa, Ó. Monroig, Methyl-end desaturases with Δ12 and ω3 regioselectivities enable the *de novo* PUFA biosynthesis in the cephalopod Octopus vulgaris, *BBA–Mol*, Cell Biol. L. 186 (2019) 1134–1144.
[8] Ó. Monroig, F. Hontoria, I. VarÓ, D.R. Tocher, J.C. Navarro, Investigating the essential fatty acids in the common cuttlefish *Sepia officinalis* (Mollusca, Cephalopoda): molecular cloning and functional characterisation of fatty acyl desaturase and elongase, Aquaculture 450 (2016) 38–47.
[9] M.Z. Li, K.S. Mai, G. He, Q.H. Ai, W.B. Zhang, W. Xu, J. Wang, Z.G. Liufu, Y. J. Zhang, H.H. Zhou, Characterization of two Δ5 fatty acyl desaturases in abalone (*Haliotis discus hannai Ino*), Aquaculture 416-417 (2013) 48–56.
[10] H.L. Liu, H.P. Zheng, S.Q. Wang, Y.J. Wang, S.K. Li, W.H. Liu, G.F. Zhang, Cloning and functional characterization of a polyunsaturated fatty acid elongase in a marine bivalve noble scallop, Aquaculture 416-417 (2013) 146–151.
[11] H.L. Liu, H.K. Zhang, H.P. Zheng, S.Q. Wang, Z.C. Guo, G.F. Zhang, PUFA biosynthesis pathway in marine scallop, J. Agric. Food Chem. 62 (2014) 12384–12391.
[12] H.L. Liu, Z.C. Guo, H.P. Zheng, S.Q. Wang, Y.J. Wang, W.H. Liu, G.F. Zhang, Functional characterization of a Δ5-like fatty acyl desaturase and its expression during early embryogenesis in the noble scallop *Chlamys nobilis Reeve*, Mol. Biol. Rep. 41 (2014) 7437–7445.
[13] H.K. Zhang, H.L. Liu, D.X. Cheng, H.X. Liu, H.P. Zheng, Molecular cloning and functional characterisation of a polyunsaturated fatty acid elongase in a marine bivalve *Crassostrea angulate*, J. Food Nutr. Res. 6 (2018) 89–95.
[14] K.B. Wu, Z.S. Ran, S.R. Wu, H.X. Xie, Y.R. Li, K. Liao, J.L. Xu, X.J. Yan, Biosynthesis of LC-PUFA in *Ruditapes philippinarum*: cloning and tissue distribution of Fad and Elovl, and effects of microalgae diets varied in LC-PUFA composition on their expressions and fatty acids profile of this bivalve, Front. Mar. Sci. 10 (2023) 1141231.
[15] Z.S. Ran, F. Kong, J.L. Xu, K. Liao, X.J. Yan, Transcriptional regulation mechanism of sterol regulatory element binding proteins on Δ6 fatty acyl desaturase in razor clam *Sinonovacula constricta*, Brit. J. Nutr. 124 (2020) 881–889.
[16] Y.L. Guo, D. Huang, F.Y. Chen, S.L. Ma, W.Y. Zhou, W.B. Zhang, K.S. Mai, Lipid deposition in abalone *Haliotis discus hannai* affected by dietary lipid levels through AMPKα2/PPARα and JNK/mTOR/SREBP-1c pathway, Aquaculture 532 (2021) 736040.
[17] J.N. Lee, H. Kim, H. Yao, Y. Chen, K. Weng, J. Ye, Identification of Ubxd8 protein as a sensor for unsaturated fatty acids and regulator of triglyceride synthesis, P. Natl. Acad. Sci. 107 (2010) 21424–21429.
[18] J.N. Lee, X. Zhang, J.D. Feramisco, Y. Gong, J. Ye, Unsaturated fatty acids inhibit proteasomal degradation of Insig-1 at a postubiquitination step, J. Biol. Chem. 283 (2008) 33772–33783.
[19] H. Kim, H. Zhang, D. Meng, G. Russell, J.N. Lee, J. Ye, UAS domain of Ubxd8 and FAF1 polymerizes upon interaction with long-chain unsaturated fatty acids, J. Lipid Res. 54 (2013) 2144–2152.
[20] R.A. DeBose-Boyd, J. Ye, SREBPs in lipid metabolism, insulin signaling, and beyond, Trends Biochem. Sci. 43 (2018) 358–368.
[21] A. Buchberger, From UBA to UBX: new words in the ubiquitin vocabulary, Trends Cell Biol. 12 (2002) 216–221.
[22] Z.S. Ran, Z.Z. Li, X.J. Yan, K. Liao, F. Kong, L. Zhang, J.Y. Cao, C.X. Zhou, P. Zhu, S. He, W.L. Huang, J.L. Xu, Chromosome-level genome assembly of the razor clam *Sinonovacula constricta* (Lamarck, 1818), Mol. Ecol. Resour. 19 (2019) 1647–1658.
[23] Z.S. Ran, S. Li, R.T. Zhang, J.L. Xu, K. Liao, X.J. Yu, Y.Y. Zhong, M.W. Ye, X.J. Yan, Fatty acid and sterol changes in razor clam *Sinonovacula constricta* (Lamarck 1818) reared at different salinities, Aquaculture 473 (2017) 493–500.
[24] Z.S. Ran, J.L. Xu, K. Liao, S. Li, S.B. Chen, X.J. Yan, Biosynthesis of polyunsaturated fatty acids in the razor clam *Sinonovacula constricta*: characterization of Δ5 and Δ6 fatty acid desaturases, J. Agr. Food Chem. 66 (2018) 4592–4601.
[25] Z.S. Ran, J.L. Xu, K. Liao, Ó. Monroig, J.C. Navarro, A. Oboh, M. Jin, Q.C. Zhou, C. X. Zhou, D.R. Tocher, X.J. Yan, Biosynthesis of long-chain polyunsaturated fatty acids in the razor clam *Sinonovacula constricta*: characterization of four fatty acyl elongases and a novel desaturase capacity, BBA−Mol, Cell Biol. L. 1864 (2019) 1083–1090.
[26] M.A. Larkin, G. Blackshields, N.P. Brown, R. Chenna, P.A. McGettigan, H. McWilliam, F. Valentin, I.M. Wallace, A. Wilm, R. Lopez, J.D. Thompson, T. J. Gibson, J.D. Thompson, Clustal W and Clustal X version 2.0, Bioinformatics 23 (2007) 2947–2948.
[27] S. Kumar, G. Stecher, K. Tamura, MEGA7: molecular evolutionary genetics analysis version 7.0 for bigger datasets, Mol. Biol. Evol. 33 (2016) 1870–1874.
[28] C.W. Wang, S.C. Lee, The ubiquitin-like (UBX)-domain-containing protein Ubx2/Ubxd8 regulates lipid droplet homeostasis, J. Cell Sci. 125 (2012) 2930–2939.
[29] K.J. Livak, T.D. Schmittgen, Analysis of relative gene expression data using real time quantitative PCR and the $2^{-\Delta\Delta CT}$ method, Methods 25 (2001) 402–408.
[30] I. Wittig, H.P. Braun, H. Schägger, Blue native PAGE, Nat. Protoc. 1 (2006) 418–428.
[31] D.D. Feng, Q. Li, H. Yu, RNA interference by ingested dsRNA-expressing bacteria to study shell biosynthesis and pigmentation in *Crassostrea gigas*, Marine Biotechnol. 21 (2019) 526–536.
[32] B.Y. Hu, Q. Li, H. Yu, RNA interference by ingested dsRNA-expressing bacteria to study porphyrin pigmentation in *Crassostrea gigas*, Int. J. Mol. Sci. 22 (2021) 6120.
[33] Y.H. Wang, X.M. Zhu, S.S. Lian, Y.R. Li, N.N. Hu, X.L. Hu, Z.M. Bao, S. Wang, Functional characterization of Cfap206 for bivalve ciliogenesis by RNAi and CRISPR/Cas9 technologies, Front. Mar. Sci. 9 (2022) 864037.
[34] E.G. Bligh, W.J. Dyer, A rapid method lipid extraction and purification, Can. J. Biochem. Physiol. 37 (1959) 911–917.
[35] Z.S. Ran, F. Kong, J.L. Xu, K. Liao, X.R. Xu, P. Shi, K. Chen, C.X. Zhou, X.J. Yan, Fad and Elovl expressions, fatty acid compositions, and feed effects of three representative microalgae in *Sinonovacula constricta* (Lamarck 1818) at early developmental stages, Aquaculture 521 (2020) 735101.
[36] A. Voss, M. Reinhart, S. Sankarappa, H. Sprecher, The metabolism of 7, 10, 13, 16, 19-docosapentaenoic acid to 4, 7, 10, 13, 16, 19-docosahexaenoic acid in rat liver is independent of a 4-desaturase, J. Biol. Chem. 266 (1991) 19995–20000.
[37] J.L. Xu, H.B. Zhou, X.J. Yan, C.X. Zhou, P. Zhu, B. Ma, Effect of unialgal diets on the composition of fatty acids and sterols in juvenile Ark shell *Tegillarca granosa Linnaeus*, J. Agric. Food Chem. 60 (2012) 3973–3980.
[38] J.X. Zhang, Z.S. Ran, H.X. Xie, F. Kong, M.Q. Zhang, Y. Zhou, Y.R. Li, K. Liao, X. J. Yan, J.L. Xu, A systematic analysis and evaluation of nutritional composition of 23 strains of marine microalgae commonly used in aquaculture, Algal Res. 72 (2023) 103122.
[39] F. Kong, Z.S. Ran, H. Xie, X.X. Tian, K. Liao, J.L. Xu, Effects of three microalgal diets varying in LC-PUFA composition on growth, Fad, and Elovl expressions, and fatty acid profiles in juvenile razor clam *Sinonovacula constricta*, Fishes 8 (2023) 484.